# THE EFFECT OF THE MODE OF COOLING ON SIZE DISTRIBUTION OF CRYSTALS PRODUCED IN BATCH CRYSTALLIZER

J. NÝVLT

*Institute of Inorganic Chemistry, 400 60 Ústí nad Labem*

Received November 23rd, 1973

Mathematical model is proposed of an agitated batch crystallizer and the effect of the form of cooling on size distribution of product crystals is evaluated on a digital computer. Studied forms of cooling were: cooling without a control, controlled cooling with linear temperature decrease, and temperature decrease with the third and fourth powers of time — both latter mentioned cases resulted from the theoretical solution of a batch crystallizer. It was determined that the time dependence of supersaturation and, consequently, the size distribution of product crystals as well depended to a great extent on the mode of cooling of the batch crystallizer. For cooling corresponding to theoretical relations, an expressive dependence on the initial supersaturation of the solution has been found.

Very few papers have been dedicated so far to the study of size distribution of crystals produced in a batch crystallizer.

Review of theoretical relations[1] as well as an analysis of experimental data[2] have been published. One of the most important limitation of the general validity of the obtained relations is the assumption of constant supersaturation within the controlled crystallization operation. Reliable information on the actual time dependence of supersaturation are not yet available due to difficulties with the experimental measurement of small supersaturations during crystallization. Here, an effort is made to obtain clear ideas on time dependences of supersaturation at various modes of cooling of a batch crystallizer and on how this dependence will affect some of directly measurable quantities, *e.g.* the size distribution of crystals produced.

For formulation of the mathematical model of a mixed batch crystallizer, differential equations are being applied for the kinetics of individual operations, *i.e.* nucleation and crystal growth

$$\dot{m}_N = k_N \Delta w^n , \qquad (1)$$

$$\dot{m}_G = k_G A \Delta w^g . \qquad (2)$$

The material balance of supersaturation will thus have the form

$$\mathrm{d}\,\Delta w/\mathrm{d}t = s - k_G A\,\Delta w^g - k_N\,\Delta w^n\,, \qquad (3)$$

where all quantities are related to a unit amount of suspension. With regard to the definition of concentration ($w$ = kg of crystallizing substance/kg of free solvent), the unit amount of suspension or solution is the amount containing 1 kg of free solvent.

Surface area of crystals can be calculated from their number and size, both these quantities being functions of time and supersaturation:

$$A = \beta N_0(L_0 + \int_0^t \dot{L}\mathrm{d}t)^2 + \int_0^t \beta N(L_N + \int_{t_N}^t \dot{L}\mathrm{d}t)^2\,\mathrm{d}t\,, \qquad (4)$$

where the limit of integration $t_N$ represents the time in which nucleation of corresponding crystals took place. Solution of this Eq. or of its combination with the initial relation (3) must be made iteratively, similarly as for the continuous crystallizer[3]. Calculation procedure is explained in the appendix.

For calculation of basical dependences on the computer Tesla 200, calculations of the crystallization operation were made for various modes of cooling with the system constants valid approximately for non-seeded aqueous solutions of ammonium sulphate: $n = 4{\cdot}9$; $k_{NO} = 1{\cdot}10^6$, $g = 1{\cdot}0$; $k_{GO} = 0{\cdot}12$; $E_G = E_N = 0$; $m_0 = 0$; $L_0 = 1{\cdot}10^{-4}$ m; $L_N = 1{\cdot}2\,.\,10^{-4}$ m; $\alpha = 1$; $\beta = 6$; $w_0 = 2{\cdot}83$; $E_w = 776{\cdot}2$; $\varrho_c = 1\,770$ kg/m$^3$. For tuning of the programme 12 seconds were chosen as the satisfying length of the time interval so that to a two-hour programme corresponds $t_e = 600$, four-hour $t_e = 1\,200$ *etc*; kinetic constants $k_{GO}$ and $k_{NO}$ were also adapted to this time unit. For initial and final crystallization temperatures were chosen $T_0 = 60°C$, $T_e = 45°C$. Value of the constant characterizing mass transfer at non-controlled cooling was chosen $K = 1{\cdot}11\,.\,10^{-3}$ or $0{\cdot}556\,.\,10^{-3}$, temperature of the cooling water was $T_w = 25°C$. Survey of computerized examples is presented in Table I.

## RESULTS AND DISCUSSION

In all thirteen experiments the time dependences of supersaturation and the granulometric product composition (differential and cumulative curves) were calculated. Results of calculations are plotted in Figs 1 to 12 with the curves numbered in the same manner as data in Table I.

In Figs 1 and 2 the time dependence of supersaturation for experiments with the comparable time of cooling and for different modes of cooling is plotted. From these two Figs it is obvious that the non-controlled or linear cooling gives very similar dependence of supersaturation with a significant maximum corresponding to the boundary of the metastable region soon after the experiment has been started. Thus, as the result sudden nucleation might be expected at the beginning of the operation

with its slower rate in the next stages so that a very fine product with a greater slope of the distributing curve should result. The effect of cooling rate for linear cooling is clearly represented in Fig. 3: The greater is the cooling rate, the faster is reached the boundary of the metastable region, corresponding to higher supersaturations, which fully corresponds to the results obtained earlier[4].

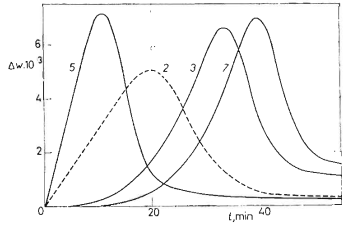


FIG. 1

Dependence of Supersaturation on Time for Different Modes of Cooling and Total Time of Experiment 1 h

Dashed curve is that from Exp. 2 in which the total time of experiment exceeds 3 h. The curves are numbered in the same manner as data in Table I.

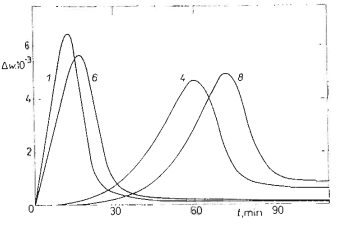


FIG. 2

Dependence of Supersaturation on Time for Different Modes of Cooling and Total Time of Experiment 2 h

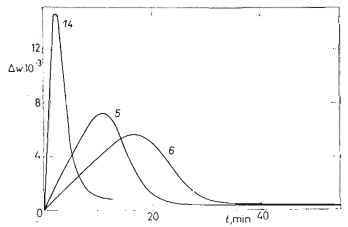


FIG. 3

Dependence of Supersaturation on Time for Linear Cooling at Different Rates: *3* 15 K/h; *4* 7·5 K/h; *14* 75 K/h

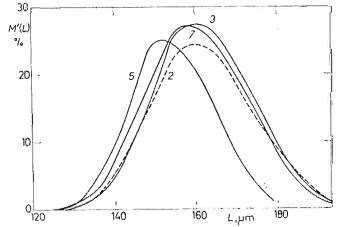


FIG. 4

Differential Granulometric Product Composition for the Experiments Given in Fig. 1

TABLE I
Initial Parameters of the Model Experiments

| Parameter | 1 | 2 | 3 | 4 | 5 | 6 |
|---|---|---|---|---|---|---|
| $X$ | 0 | 0 | 1 | 1 | 3 | 3 |
| $K$ | $1{\cdot}11 \cdot 10^{-3}$ | $5{\cdot}56 \cdot 10^{-4}$ | 0 | 0 | 0 | 0 |
| $t_e$ | 505 | 1 007 | 300 | 600 | 300 | 600 |
| $\Delta w_0$ | 0 | 0 | 0 | 0 | 0 | 0 |

Unlike in those experiments where cooling has been performed according to the theoretical relation a very slow increase in supersaturation takes place at the initial zero supersaturation up to the distinctly lower maximum appearing in about the second third of the experiment. Supersaturation then decreases and remains at an approximately constant value (higher than the corresponding value for non-controlled or linear cooling). As the maximum is smaller and the area under the

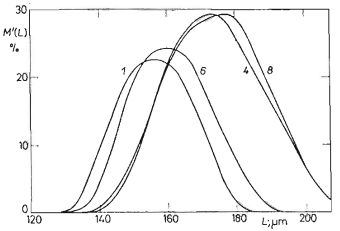


FIG. 5
Differential Granulometric Product Composition for Experiments Given in Fig. 2

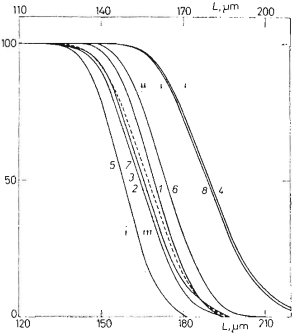


FIG. 6
Cumulative Sieve Spectra of Products from Figs 1 and 2

For Exp *2*, *3*, *5*, *7* holds the lower scale, for *1*, *4*, *6*, *8* the upper one.

TABLE I
(*Continued*)

| Experiment No | | | | | | |
|---|---|---|---|---|---|---|
| *7* | *8* | *9* | *10* | *11* | *12* | *13* |
| 4 | 4 | 4 | 4 | 4 | 4 | 4 |
| 0 | 0 | 0 | 0 | 0 | 0 | 0 |
| 300 | 600 | 600 | 600 | 600 | 600 | 600 |
| 0 | 0 | $1 . 10^{-3}$ | $2 . 10^{-3}$ | $3 . 10^{-3}$ | $4 . 10^{-3}$ | $5 . 10^{-3}$ |

curve is larger, a smaller number of originating crystals can be expected which means a greater mean crystal size.

The differential sieve analyses of products are given in Figs 4 and 5 again for comparable cooling times and various types of cooling curves. The curves are slightly asymmetric and according to expectations the position of maxima corresponding to the mean crystal size is increasing from the non-controlled cooling to that programmed

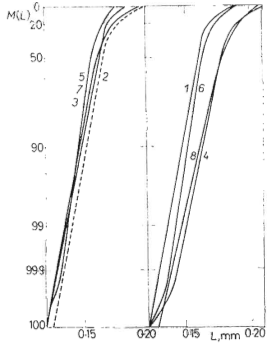


FIG. 7

Curves from Fig. 6 in Coordinates Corresponding to the Linearization at Constant Nucleation Rate

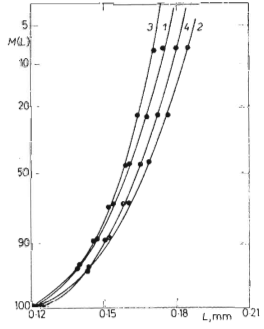


FIG. 8

Linearization of Sieve Spectra from Experiments with Non-Controlled and Constant Cooling Rate

in accordance with the theoretical relations. For higher cooling rates smaller crystals were obtained as expected.

Cumulative distribution curves of crystal sizes are in an analogical manner plotted in Fig. 6.

In one of the previously published papers[2] the granulometric product composition obtained from a batch crystallizer has been linearized at the assumption of constant supersaturation according to the relation

$$M(L) = 100[1 - (L/L_{max})^4] . \qquad (5)$$

The curves in Fig. 7 are plotted in coordinates corresponding to this linearization. The curvatures in regions of fine and coarse fractions clearly indicate the deviations from the made assumption on constant supersaturation. These deviations are quite expectable for cases of the non-controlled or linear cooling where, on the contrary, a linear dependence characteristic for batch crystallization, where supersaturation decreases exponentially could be expected[2] according to the relation

$$M(L) = 100(1 + z + z^2/2 + z^3/6) \exp(-z) , \qquad (6)$$

where $z$ is the dimensionless crystal size. Nevertheless the curves based on experiments *1—4* plotted in Fig. 8 prove that neither in these cases the decrease in supersaturation is exponential. In this case the exponential decrease in the supersaturation rate is combined here with the increase of the surface area of crystals and thus linearization according to relation (*5*) is more successful.

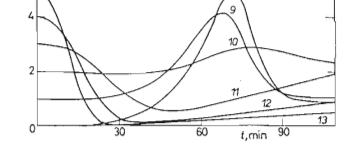


FIG. 9

Effect of Initial Supersaturation on Time Dependence of Supersaturation in Batch Crystallization

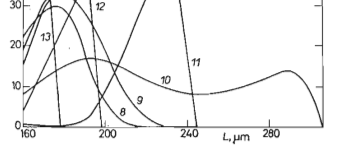


FIG. 10

Effect of Initial Supersaturation on Differential Sieve Spectra of Product

The deviations from the theoretical assumption found in experiments with $X = 4$ (and similarly with $X = 3$) can be explained by the assumption made on constant supersaturation where the corresponding experiments were made with the initial supersaturation equal to zero. In this way the defficiency of surface area of crystals in the initial stage of crystallization was responsible for the increase in supersaturation, about in the middle of the experiment, up to such value when increased nucleation rate compensated the mentioned defficiency of surface area. Of course a greater number of crystals has been formed and the new supersaturation reached at the end of the experiment is lower than the theoretical value would be. However the theoretical value is not known and its direct determination from Eqs (*3*) and (*4*) is practically impossible.

Therefore the calculation of a set of experiments *8* to *13* has been made with the increasing value of initial supersaturation from 0 up to $5 \cdot 10^{-3}$. The results are very interesting and they demonstrate a pronounced effect of initial supersaturation which could not have been expected in advance. In Fig. 9 the time dependence of supersaturation for this set of experiments is plotted.

It is obvious that in the experiments with initial supersaturation lower than the theoretical steady value (Exp. *8*, *9*), supersaturation initially increases slightly and later faster up to the maximum at the beginning of the second half of the experiment, then it relatively fastly decreases down to a constant value of about $\Delta w = 1 \cdot 10^{-3}$. On the contrary, in the experiments with initial supersaturation higher than the theoretical value (Exp. *11* to *13*) a relatively fast decrease in supersaturation takes place which is reaching the minimum value which is the lower and reached the faster, the higher is the initial supersaturation, and then it slowly increases. The rate of this

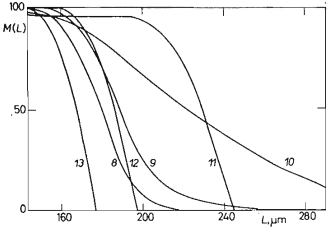


FIG. 11

Effect of Initial Supersaturation on the Shape of Cumulative Curve of Granulometric Product Composition

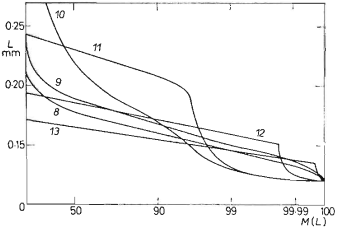


FIG. 12

Effect of Initial Supersaturation on Shape of Linearized Sieve Spectra

increase is the slower the higher is the initial supersaturation, which is the logical result based on the number and the corresponding surface area of crystals. In the Exp. *10* the value of the constant steady supersaturation was fixed with sufficient accuracy (the theoretical value is expected to be even slightly higher) and the supersaturation is – as anticipated – in the whole experiment about constant with insignificant maximum in the second half of the experiment.

The different character of the time dependence of supersaturation must of course affect the granulometric product composition (Figs 10–12). The granulometric product compositions with initial supersaturation lower than is the theoretical value are about symmetrically distributed in respect to the size most frequently present, the maximum is moving with increasing supersaturation slightly toward larger crystal sizes. At the supersaturation close to the theoretical value (curve *10*) the character of granulometric composition changes significantly: the curve has two peaks and it seems that nucleation took place at about a constant rate during the whole experiment (this is most obvious in Fig. 11). At initial supersaturations higher than the theoretical value the two-peak character again disappears, the curve is assymetric, with a relatively large slope, for the product in Exp. *11* with an insignificant portion of small crystals down to sizes of nuclei.

The position of maximum moves with increasing initial supersaturation backward to smaller crystal sizes. It is interesting that more uniform composition of products has been obtained with larger initial supersaturations. Explanation can be found in nucleation taking place mainly at the beginning of the operation while during the operation the crystal growth mostly took place.

## CONCLUSIONS

The applied mathematical model described in an adequate manner the behaviour of a batch crystallizer and thus enabled to study sensitively the effect of individual factors on batch crystallization. The results of the model calculation based on the data of the system ammonium sulphate–water without seeding have demonstrated that – as anticipated – non-controlled and linear cooling resulted in a considerable nucleation at the beginning of the operation, with supersaturation then decreasing to a very low value and products in both these cases consisted of fine particles. The programmed cooling according to the theoretical curves results in a visible improvement of the product. In number of cases supersaturation is reaching its maximum in the second half of the experiment and it steadies at a given value higher than for the noncontrolled cooling at the end. A considerable dependence on the initial supersaturation has been found. The optimum results can be obtained when the value of the initial supersaturation is fixed slightly higher than the initial supersaturation corresponding to steady value under the given conditions. The determination and operation of an industrial crystallizer at this steady value will be very difficult. Nevertheless to obtain a high

quality product it is not unconditionally necessary to keep the inital supersaturation at an accurate value but it suffices to approach it as closely as possible.

*The author wishes to thank Dr Z. Křivský and Mrs E. Langová for carrying out the computations.*

APPENDIX

Procedure for Solving the Model of a Batch Crystalliser

After reading the inlet data, the initial surface area and the number of seeded crystals are computed

$$A_0 = \beta N_0 L_0^2 , \tag{A1}$$

$$N_0 = m_0/(\alpha \varrho_c L_0^3) . \tag{A2}$$

In the next step it is necessary to specify the mode of cooling. For non-controlled cooling the cooling curve is approximated[4] by the relation

$$T = T_w + (T_0 - T_w) \exp(-Kt) , \tag{A3}$$

and for controlled cooling the cooling curve can be expressed by equation[1,2]

$$T = T_0 - (T_0 - T_e)(t/t_e)^X , \tag{A4}$$

where the value of the exponent $X$ can be $X = 1$ for linear cooling, $X = 3$ for approximation of cooling of a seeded crystallizer without nucleation and $X = 4$ for an approximation of the cooling curve of a non-seeded crystallizer with nucleation.

By use of the so determined temperature, the values of kinetic constants of growth and nucleation and also the equilibrium solubility are calculated

$$k_G = k_{GO} \exp(-E_G/\boldsymbol{R}(T + 273)) , \tag{A5}$$

$$k_N = k_{NO} \exp(-E_N/\boldsymbol{R}(T + 273)) , \tag{A6}$$

$$w_{eq} = w_0 \exp(-E_w/\boldsymbol{R}(T + 273)) . \tag{A7}$$

The supersaturation rate is defined as the change in solubility per unit of time

$$s = w_{eq(t-1)} - w_{eqt} \tag{A8}$$

so that the actual supersaturation in time is

$$\Delta w_t = \Delta w_{t-1} + \Delta(\Delta w) , \tag{A9}$$

where the change in supersaturation in the given time unit can be calculated from the basical Eq. (3)

$$\Delta(\Delta w) = s - k_G A \, \Delta w^g - k_N \Delta w^n . \tag{A10}$$

If the length of the time interval is chosen inappropriately (the step is too long) an instability of the solution can be met with values starting to oscillate with a growing amplitude till some of them reaches negative values in which case the computation must be stopped. If the supersaturation value is realistic the number of newly formed crystals is calculated from

$$N_t = k_N \Delta w^n / (\alpha \varrho_c L_N^3) \qquad (A11)$$

and the linear crystallization rate from

$$\dot{L} = k_G \beta \Delta w^g / (3\alpha \varrho_c) \qquad (A12)$$

corresponding to the given value of supersaturation. All the crystals present in the suspension will now grow on by the value $\dot{L}$

$$\begin{aligned} L_{0t} &= L_{0,t-1} + \dot{L}, \\ L_{it} &= L_{i,t-1} + \dot{L}, \\ L_j &= L_{N'} \end{aligned} \qquad (A13)$$

and in the corresponding manner also the mass of individual fractions is rising as well

$$\begin{aligned} m_{0t} &= N_0 \alpha \varrho_c L_{0t}^3, \\ m_{it} &= N_i \alpha \varrho_c L_{it}^3, \\ m_t &= m_{0t} + \sum m_{it}. \end{aligned} \qquad (A14)$$

Surface area of crystals is then

$$A = \beta m_0 / (\alpha \varrho_c L_0) + \sum_i \beta N_i L_i^2 . \qquad (A15)$$

As long as the time and temperature have not exceeded the required final temperature, the calculation is returned back to the calculation of temperature according to Eq. (*A3*) or (*A4*) and calculation is repeated for another time unit. After reaching the final values the product crystals must be separated into the chosen number of fractions *j e.g.* according to the relations of the type

$$\Delta L = (L_{0t_e} - L_N)/j , \qquad (A16)$$

$$L_N + k \Delta L \leqq L < L_N + (k-1) \Delta L ; \quad k \in \langle 0, j \rangle ,$$

and masses of individual fractions as well as their total masses must be summed. Finally the differential and cumulative granulometric product compositions are computed

$$M'(L_j) = 100 m_j / \sum_j m_j , \qquad (A17)$$

$$M(L_j) = \sum_{j=0}^{j} M'(L_j) . \qquad (A18)$$

LIST OF SYMBOLS

| | |
|---|---|
| $A$ | surface area of crystals ($m^2/kg_0$; $kg_0$ represents 1 kg of free solvent) |
| $A_0$ | surface area of crystals seeded ($m^2/kg_0$) |
| $E_N$ | activation energy of nucleation (kcal/kmol) |
| $E_G$ | activation energy of crystal growth (kcal/kmol) |
| $E_w$ | parameter of energy characterizing the temperature dependence of solubility (kcal/kmol) |
| $g$ | order of kinetic equation of growth |
| $k_N$ | rate constant of nucleation ($kg_0^{n-1}\ kg^{1-n}\ s^{-1}$) |
| $k_G$ | rate constant of growth ($kg^{1-g}\ m^{-2}\ s^{-1}\ kg_0^g$) |
| $k_{NO}$ | constant in Eq. (*A6*) ($kg_0^{n-1} kg^{1-n}\ s^{-1}$) |
| $k_{GO}$ | constant in Eq. (*A5*) ($kg^{1-g}\ m^{-2}\ s^{-1}\ kg_0^g$) |
| $K$ | constant characterizing heat transfer |
| $L$ | crystal size (m) |
| $L_0$ | size of seeded crystals (m) |
| $L_N$ | size of crystal nuclei (m) |
| $L_{max}$ | size of largest crystals in the product (m) |
| $\dot{L}$ | linear crystallization rate (m/s) |
| $M(L)$ | cumulative granulometric distribution (oversize fraction) |
| $M'(L)$ | differential granulometric distribution (%) |
| $\Delta m$ | mass of crystals formed in a batch ($kg/kg_0$) |
| $m_0$ | mass of crystals seeded ($kg/kg_0$) |
| $\dot{m}_G$ | mass rate of crystal growth ($kg\ kg_0^{-1}\ s^{-1}$) |
| $\dot{m}_N$ | mass rate of nucleation ($kg\ kg_0^{-1}\ s^{-1}$) |
| $n$ | order of kinetic equation of nucleation |
| $N_0$ | number of crystals seeded ($kg_0^{-1}$) |
| $\dot{N}$ | numerical nucleation rate ($kg_0^{-1}\ s^{-1}$) |
| $R$ | gas constant (kcal/kmol K) |
| $s$ | supersaturation rate ($kg\ kg_0^{-1}\ s^{-1}$) |
| $t$ | number of time intervals |
| $T$ | temperature (°C) |
| $T_0$ | initial temperature (°C) |
| $T_e$ | final temperature (°C) |
| $T_w$ | temperature of cooling water (°C) |
| $-\dot{T}$ | cooling rate (K/s) |
| $w$ | concentration ($kg/kg_0$) |
| $w_0$ | constant in Eq. (*A7*) ($kg/kg_0$) |
| $\Delta w$ | supersaturation ($kg/kg_0$) |
| $w_{eq}$ | solubility ($kg/kg_0$) |
| $X$ | exponent in equation of the cooling curve (*A4*) |
| $z$ | dimensionless crystal size |
| $\alpha$ | volume shape factor |
| $\beta$ | surface area shape factor |
| $\varrho_c$ | density of crystals ($kg/m^3$) |

Subscripts

| | |
|---|---|
| *i* | crystals formed in time *i* |
| *j* | class of crystal sizes |
| *t* | value in time *t* |
| *e* | final value |

REFERENCES

1. Nývlt J., Kočová H., Černý M.: This Journal *38*, 3199 (1973).
2. Nývlt J.: Chem. průmysl *23*, 343 (1973).
3. Nývlt J., Mullin J. W.: Chem. Eng. Sci. *25*, 131 (1970).
4. Nývlt J.: This Journal *28*, 2269 (1963).

Translated by M. Rylek.